# Impact of vertical mixing on sea surface pCO2 in temperate seasonally stratified shelf seas

Rippeth, T.P.; Lincoln, B.J.; Kennedy, H.A.; Palmer, Matthew; Sharples, J.; Williams, C.A.

**Journal of Geophysical Research: Oceans**

*DOI:*
10.1002/2014JC010089

Published: 20/06/2014

Publisher's PDF, also known as Version of record

AGU PUBLICATIONS

JGR

Journal of Geophysical Research: Oceans

RESEARCH ARTICLE

10.1002/2014JC010089

**Key Points:**
- Diapycnal fluxes in seasonally stratified shelf seas impact on air-sea $CO_2$ fluxes
- Surface mixing layer depth and turbulent dissipation within the thermocline and C:N uptake ratio by phytoplankton are key parameters in determining the impact of mixing
- Episodic wind events may play a key role in driving air-sea $CO_2$ fluxes in these regions

**Correspondence to:**
T. P. Rippeth,
t.p.rippeth@bangor.ac.uk

**Citation:**
Rippeth, T. P., B. J. Lincoln, H. A. Kennedy, M. R. Palmer, J. Sharples, and C. A. J. Williams (2014), Impact of vertical mixing on sea surface $pCO_2$ in temperate seasonally stratified shelf seas, *J. Geophys. Res. Oceans*, *119*, 3868–3882, doi:10.1002/2014JC010089.

Received 24 APR 2014
Accepted 20 MAY 2014
Accepted article online 3 JUN 2014
Published online 20 JUN 2014



# Impact of vertical mixing on sea surface $pCO_2$ in temperate seasonally stratified shelf seas

**T. P. Rippeth[1], B. J. Lincoln[1], H. A. Kennedy[1], M. R. Palmer[2], J. Sharples[2,3], and C. A. J. Williams[3]**

[1]School of Ocean Sciences, Bangor University, Anglesey, Wales, UK, [2]National Oceanography Centre, Liverpool, UK, [3]School of Environmental Sciences, University of Liverpool, Liverpool, UK

**Abstract** A key parameter in determining the exchange of $CO_2$ across the ocean-atmosphere interface is the sea surface partial pressure of carbon dioxide ($pCO_2$). Temperate seasonally stratified shelf seas represent a significant sink for atmospheric $CO_2$. Here an analytical model is used to quantify the impact of vertical mixing across the seasonal thermocline on $pCO_2$. The model includes the impacts of the resultant dissolved inorganic carbon, heat, salt, and alkalinity fluxes on the solubility of $CO_2$ and the effect of the inorganic carbon sink created by the primary production fuelled by the flux of limiting nutrient. The results indicate that diapycnal mixing drives a modest but continuous change in $pCO_2$ of order 1–10 μatm $d^{-1}$. In quantifying the individual impacts of the fluxes of the different parameters, we find that the impact of the fluxes of DIC and nitrate fluxes dominate. In consequence, both the direction and magnitude of the change in $pCO_2$ are strongly dependent on the C:N uptake ratio in primary production. While the smaller impacts of the heat and salt fluxes tend to compensate for each other at midshelf locations, the heat flux dominates close to the shelf break. The analysis highlights the importance of the accurate parameterization of the C:N uptake ratio, the surface-mixed layer depth, and the TKE dissipation rate within the seasonal thermocline in models to be used to predict the air-sea exchange of carbon dioxide in these regimes. The results implicate storms as key periods of $pCO_2$ perturbation.

## 1. Introduction

Continental shelf seas play a key role in the global carbon cycle, linking the terrestrial, marine, and atmospheric carbon reservoirs [*Walsh*, 1991; *Bauer et al*., 2013]. Although they account for only 7% of the surface area of the ocean, they are estimated to account for 10–30% of global oceanic primary production, 30–50% of inorganic carbon, and around 80% of organic carbon burial [*Bauer et al*., 2013]. In consequence, shelf seas host significant fluxes of $CO_2$ across the air-sea interface [e.g., *Thomas et al*., 2004; *Borges et al*., 2005; *Cai et al*., 2005], with a consensus that temperate seasonally stratified shelf seas represent a net sink for atmospheric $CO_2$ [*Chen and Borges*, 2009]. A key parameter in determining the fluxes of $CO_2$ between the shelf seas and the atmosphere is the sea surface $pCO_2$. Oversaturation of $pCO_2$ relative to the atmosphere leads to outgassing, while undersaturation leads to the uptake of $CO_2$ from the atmosphere by the ocean. The relative magnitudes of $CO_2$ outgassing and uptake over the annual cycle determines whether the shelf sea represents a net source or sink. A significant proportion of the variability of sea surface $pCO_2$ in seasonally stratified shelf seas is attributed to primary productivity [*Wakelin et al*., 2012].

The presence of nutrients in the euphotic zone fuels primary production, with the net removal of inorganic carbon, resulting in a pH increase and a decrease in $pCO_2$ potentially leading to $CO_2$ undersaturation. In contrast, when respiration dominates, e.g., during the remineralization of organic matter in the dark, $pCO_2$ increases. In seasonally stratified shelf seas, the zones where primary production and respiration dominate are separated by a seasonal thermocline. Primary production in the surface-mixed layer results in a net flux of organic carbon across the thermocline into the deep water where it is remineralized. The seasonally integrated balance of these processes suggests that temperate seasonally stratified shelf seas such as the North Sea are significant net sinks for atmospheric $CO_2$ [*Thomas et al*., 2004; *Bozec et al*., 2006; *Evans et al*., 2012; *Kitidis et al*., 2012].

Primary production in the ocean is often viewed as being dominated by the spring bloom. However, once the spring bloom has exhausted the nutrients in the surface-mixed layer, a key process responsible for sustaining primary productivity during the summer months is the introduction of the deep water nutrients via

diapycnal turbulent mixing across the thermocline [*Sharples and Tett*, 1994; *Sharples et al*., 2001; *Williams et al*., 2013a, 2013b]. The manifestation of this mixing is the development of a subsurface chlorophyll maximum.

The subsurface chlorophyll maximum (SCM) has been estimated to account for up to 50% of annual carbon fixation in these regions [*Richardson et al*., 2000; *Rippeth et al*., 2009; *Weston et al*., 2005; *Hickmann et al*., 2012; *van Leeuwen et al*., 2013] with enhanced SCM productivity noted over rough topography [*Fernand et al*., 2013]. Studies of the seasonal dynamics of the shelf sea $CO_2$ system, at a seasonally stratified site in the English Channel, showed that monthly mean surface water $pCO_2$ is strongly inversely correlated with the depth integrated chlorophyll, but not with the surface chlorophyll [*Kitidis et al*., 2012]. These observations therefore suggest that the SCM plays a critical role in determining $CO_2$ uptake at this site [*Kitidis et al*., 2012], thus implicating diapycnal mixing as a key process in controlling air-sea $CO_2$-fluxes in temperate seasonally stratified shelf seas. Recent simulations using coupled shelf sea hydrodynamic-ecosystem models underestimate primary production within the SCM [*van Leeuwen et al*., 2013] with the underestimation of diapycnal mixing rates identified as a potential contributory factor in the reported error in predicted air-sea $CO_2$ flux estimates for these locations [*Artioli et al*., 2012; *Wakelin et al*., 2012].

The aim of this paper is to investigate the impact of diapycnal mixing on the sea surface $pCO_2$ in seasonally stratified shelf seas. To achieve this, we quantify the impact of the nitrate flux across the seasonal thermocline, for a range a contrasting sites in the northwest European shelf seas, using a one-dimensional turbulent diffusion model, and compare it to the potentially compensatory impacts of the accompanying fluxes of dissolved inorganic carbon (DIC), heat, alkalinity, and salt. We also investigate the impact of hydrodynamic parameters; the surface-mixed layer depth and the rate of diapycnal mixing; and a biogeochemical parameter, the relative carbon to nitrogen uptake ratio, in primary productivity, on the surface $pCO_2$.

## 2. Processes Driving Diapycnal Turbulent Mixing Within the Seasonal Thermocline

The first-order paradigm for water column structure in the Northwest European shelf seas is well established as resulting from the balance between buoyancy input at the sea surface, by solar heating, and turbulent mixing driven largely by the tides [*Simpson and Hunter*, 1974]. Over 70% of the region is subject to seasonal stratification, with warmer water overlying cooler water from spring through until the autumn. Thus, surface and deep water layers are separated by a pycnocline, across which exchange of water and hence fluxes of scalars, are a result of turbulent mixing. The temperature variation in temperate seasonally stratified continental shelf seas is dominated by the seasonal cycle. In the North Sea, the seasonal cycle explains 96% of the observed temperature variance [*Howarth et al*., 1992] with interannual variability primarily influenced by the local meteorology rather than advection of water from the adjacent NE Atlantic [*Sharples et al*., 2006]. This implies that vertical exchange processes are the first-order determinant of the water column structure in the Northwest European shelf seas. Despite the remoteness of much of the seasonally stratified North Sea from the main regions of freshwater influence in the southern North Sea, the thermal stratification in this region is often augmented by haline stratification [*Howarth et al*., 1992].

Examples of water column profiles are shown in Figure 2 for a range of contrasting seasonally stratified locations in the Northwest European shelf seas (as identified in Figure 1). They typically show warmer, and in some cases fresher water, overlying cooler (saltier) water with a surface-mixed layer depth of 10–40 m. In each case, the surface-mixed layer is nitrate depleted following the spring bloom, while significant nitrate concentrations are observed in the water below the pycnocline. A ubiquitous feature of the seasonally stratified shelf seas is the subsurface chlorophyll maximum (SCM) which is observed within the pycnocline region of each of the profiles and is sustained by the diapycnal nutrient flux driven by vertical mixing coupled with adequate light availability in the region of the SCM [*Sharples and Tett*, 1994; *Williams et al*., 2013a]. In the shelf sea regions reported here, the limiting nutrient is nitrate [*Howarth et al*., 1992; *Gibson et al*., 1997; *Sharples et al*., 2001] and so we will only consider this nutrient in the analysis presented.

Numerous turbulent mixing processes have been implicated in driving diapycnal fluxes in these regimes. These processes include those arising from shear stresses associated with the sea surface and seabed boundaries and shear instability within the interior [*Stacey et al*., 2012]. The height of the bottom and top of the pycnocline is determined as the balance point between boundary generated and interior generated turbulence. In situations where the boundary forcing increases, diapycnal fluxes can result from the penetration

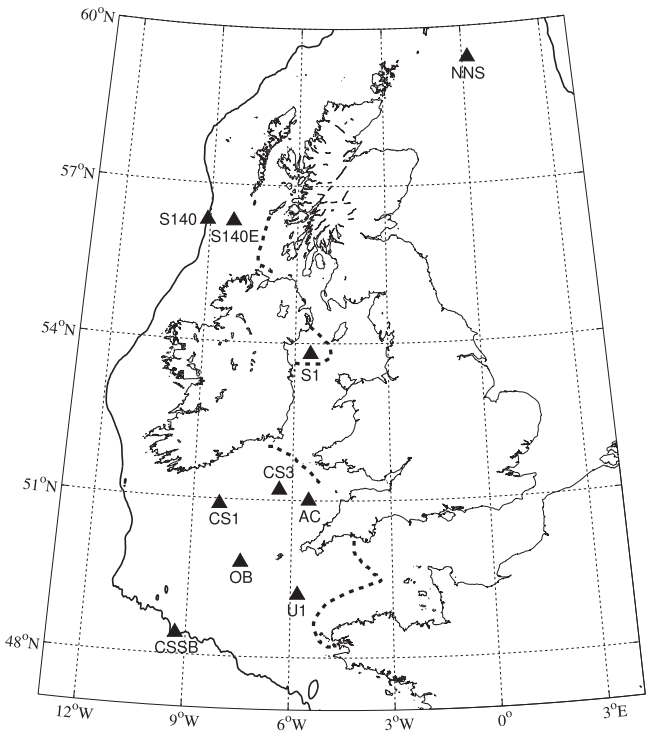


**Figure 1.** Map of the continental shelf seas to the west of Britain showing the location of the continental shelf break (200 m contour), the tidal mixing fronts (---), and the locations (▲) of the seasonally stratified stations referred to in the text.

of the boundary layer into the pycnocline gradient region. An example would be the increasing tidal boundary layer height as the tidal current strength increases from neaps to springs. *Sharples et al*. [2001] report what is believed to be such an event at a location (U1) in the English Channel.

Observations indicate that the temperate shelf sea pycnocline is often only marginally stable [*van Haren et al*., 1999; *MacKinnon and Gregg*, 2005; *Rippeth*, 2005; *Rippeth et al*., 2005] and hence additional shear across the pycnocline may result in shear instability and turbulent mixing. A number of phenomena have been observed to contribute to shear across the thermocline and by implication turbulent mixing in these regimes. They include internal tides and solitary waves generated by tidal flow over the continental shelf break [e.g., *Inall et al*., 2000; *Sharples et al*., 2007] and over continental shelf banks [*Palmer et al*., 2013a], and also wind-driven near-inertial oscillations [e.g., *Knight et al*., 2002; *Palmer et al*., 2008; *Burchard and Rippeth*, 2009; *Rippeth et al*., 2009; *Lincoln et al*., 2014]. In all cases, the level of turbulence generated is observed to be sufficiently large to drive significant fluxes across the pycnocline.

At each of the stations used in this study, time series of profiles of the rate of dissipation of turbulent kinetic energy ($\varepsilon$) have been made in addition to temperature and salinity measurements. The value of $\varepsilon$ provides an accurate proxy for the rate of turbulent mixing across the pycnocline [*Osborn*, 1980], and is given in Table 1. These values represent a temporal pycnocline average, which is based on 4–6 profiles/h, over a time period of between 1 tidal cycle and 60 h, as indicated in column 4 of Table 1.

The data presented have been collected in the region of isolated seasonal stratification in the western Irish Sea (S1), the Celtic Sea (midshelf, CS and shelf break, CSSB), the Northern North Sea (NNS), the Malin shelf, to the west of Scotland (midshelf S140E and shelf break S140) and the English Channel (U1). The data are divided between stations close to rough topography (stations 12–18) and stations at midshelf locations (stations 1–11). It is noted that all stations used in this study are far from Regions of Freshwater Influence (ROFIs) and in consequence the observed sea surface salinity is in all cases, $S > 33$ (PSS). Despite their remoteness from ROFIs, significant haline stratification is observed to argument the thermal stratification at a number of the locations shown (e.g., Figure 2).

Comparison of the different locations across the Northwest European shelf shows that values of $\varepsilon > 1 \times 10^{-4}$ Wm$^{-3}$ are generally characteristic of stations close to the shelf break (S140, CSSB) and other areas of rough topography such as seabed banks (e.g., CS1). The common observation of the depression of SST close to the shelf break is attributed to high levels of mixing observed in this region [e.g., *Sharples et al*., 2007]. There is also a high level of temporal variability in $\varepsilon$, which can be associated with the springs-neaps cycle of the tide coupled with the generation of an internal tide [e.g., *Inall et al*., 2000; *Sharples et al*., 2007]. Observations taken close to the Celtic Sea shelf break show a tidally averaged dissipation rate across the thermocline region which was 5 times higher close to a springs tide than it was at neaps (CSSB_N for neaps and CSSB_S for springs in Table 1). Similar variability in $\varepsilon$ has been reported for a location close to Malin

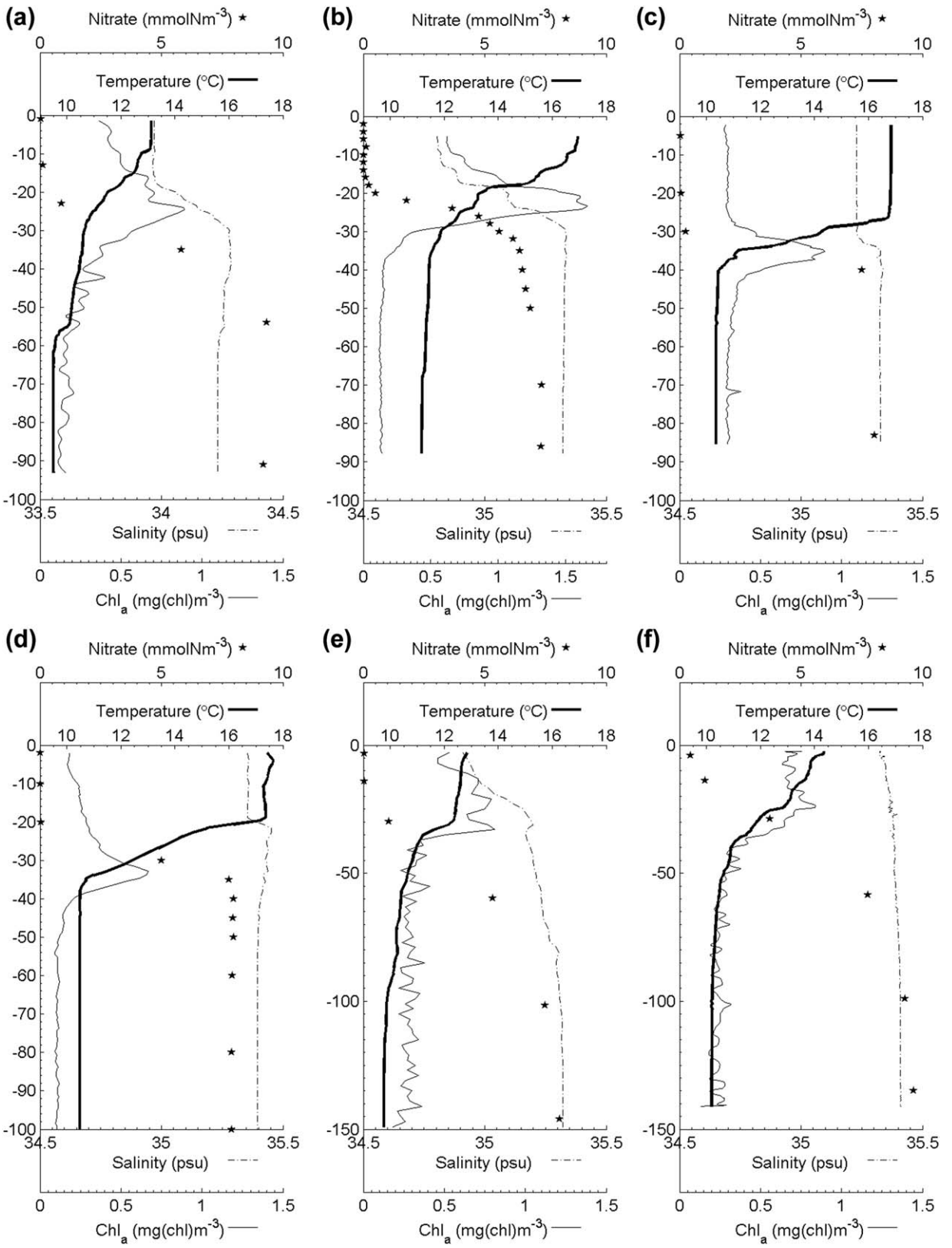


**Figure 2.** Individual profiles of water column structure for a series of contrasting locations within the seasonally stratified Northwest European shelf seas (locations are shown in Figure 1). Each represents a single CTD profile with temperature, salinity fluorescence, calibrated to show chlorophyll-a, and nitrate concentrations from water samples.(a) S1—Western Irish Sea on 26th June 2002, (b) CS3—Celtic Sea on 5th August 2003, (c) CS1—Celtic Sea on 31st July 2003, (d) OB—Celtic Sea on 2005, (e) S140E—Malin shelf on the 15th July 1996, and (f) S140—Malin shelf on the 14th July 1996.

**Table 1.** The Mean Rate of Turbulent Dissipation $<\varepsilon>$ Within the Shelf Sea Thermocline for a Series of Locations Within the Seasonally Stratified Northwest European Shelf Seas[a]

| No | Station | Date | Duration (h) | Water Depth (m) | $\varepsilon$ ($\times 10^{-4}$ W m$^{-3}$) | Reference |
|---|---|---|---|---|---|---|
| 1 | S1 | 26 Jun 2002 | 15 | 95 | 0.19 ± 0.02 | *Rippeth et al.* [2009] |
| 2 | *Ditto* | 11 Aug 1997 | 24 | 95 | 0.26 ± 0.10 | *Ditto* |
| 3 | *Ditto* | 6 July 1993 | 25 | 95 | 0.39 ± 0.12 | *Ditto* |
| 4 | CS3_I | 5 Aug 2003 | 25 | 90 | 0.67 ± 0.19 | *Palmer et al* [2008] |
| 5 | CS3_II | 10 Aug 2003 | 25 | 90 | 0.53 ± 0.09 | *Ditto* |
| 6 | OB | 1 Aug 1996 | 25 | 83 | 0.06 ± 0.03 | *Simpson and Tinker* [2009] |
| 7 | S140E_I | 15 Jul 1996 | 24 | 150 | 0.16 ± 0.01 | *Rippeth and Inall* [2002] |
| 8 | S140E_II | 23 Jul 1996 | 12.5 | 150 | 0.20 ± 0.01 | *Ditto* |
| 9 | NNS_I | 18 Oct 1998 | 60 | 110 | 0.33 ± 0.4 | *Burchard and Rippeth* [2009] |
| 10 | NNS_II | 22 Oct 1998 | 60 | 110 | 0.88 ± 0.1 | *Ditto* |
| 11 | U1 | 8 Aug 1999 | 25 | 115 | 0.6 | *Sharples et al* [2001] |
| 12 | S140_I | 14 Jul 1996 | 16 | 140 | 0.48 ± 0.04 | *Rippeth and Inall* [2002] |
| 13 | S140_II | 22 Jul 1996 | 18 | 140 | 2.11 ± 0.04 | *Ditto* |
| 14 | S140_III | 21 Aug 1995 | 12.5 | 140 | 0.37 ± 0.09 | *Inall et al* [2000] |
| 15 | S140_IV | 31 Aug 1995 | 12.5 | 140 | 1.40 ± 0.40 | *Ditto* |
| 16 | CSSB_S | 17 Jul 2005 | 25 | 190 | 3.8 | *Sharples et al* [2007] |
| 17 | CSSB_N | 23 Jul 2005 | 25 | 190 | 0.65 | *Ditto* |
| 18 | CS1 | 31 Jul 2003 | 25 (gaps) | 80 | 3.0 ± 3.0 | *Rippeth* [2005] |

[a]The Roman numeral indicates the time series number as referred to in the text. This data have been published, together with an interpretation of the physical processes driving the dissipation within the pycnocline, and thus diapycnal fluxes, in references provided. 12–18 are locations close to significant topography (i.e., a sea mount in the case of CS1 and the continental shelf break).

continental shelf break (S140_I and S140_IV are close to springs; S140_I and S140_III are close to neaps). Similar results are reported for other shelf sea areas with rough topography [*Liu et al*., 2013; *Palmer et al*., 2013b].

In general, the observed value of $\varepsilon$ at the midshelf locations (S1, CS3, OB, U1, and AC) tends to be an order of magnitude lower than those observed close to rough topography and/or the continental shelf break. Temporal variability also arises due to shear spiking resulting from the interaction between wind-driven inertial oscillations and the wind [*Rippeth et al*., 2009]. *Burchard and Rippeth* [2009] measured $\varepsilon$ values 3–4 times higher during the periods when the spiking is observed (Table 1; NNS_II represents a period with significant shear spikes, while NSS_I represents a period during which no shearing spiking was observed despite strong winds at that time). *Williams et al*. [2013b] report wind-driven pulses of nutrients across the pycnocline in the Celtic Sea in response to shear spiking which result in an enhancement of the nitrate flux by 17 times over the background level. Enhanced values for $<\varepsilon>$ have also been observed to be associated with the passage of internal solitary waves in both open shelf locations (S140) [e.g., *Inall et al*., 2000] and isolated areas of stratification such as the western Irish Sea (S1) [e.g., *Green et al*., 2010].

Assuming a local equilibrium between the rates of production of turbulent kinetic energy ($P$) and $\varepsilon$ gives

$$P = B + \varepsilon \tag{1}$$

where B is the rate at which the turbulence does work in mixing the water column (i.e., conversion of turbulent kinetic energy to water column potential energy). Using this assumption, *Osborn* [1980] derives an expression for the calculation of a turbulent diffusion coefficient

$$K_z = \frac{R_f}{1 - R_f}\left(\frac{\varepsilon}{N^2}\right) \tag{2}$$

where $N^2$ is the buoyancy frequency and $R_f$ is a flux Richardson number. Mean estimates of $K_z$, based on the observed rates of dissipation of turbulent kinetic energy, in midshelf locations, tend to lie in the region of 0.3–0.7 $\times$ $10^{-4}$ m$^2$ s$^{-1}$, and are elevated close to rough topography (1.6–6.5 $\times$ $10^{-4}$ m$^2$ s$^{-1}$). It should also be noted that $K_z$ can vary by over an order of magnitude on hourly time scales, for example, in response to inertial shear spikes or the passage of nonlinear internal waves [e.g., *Lenn et al*., 2011; *Inall et al*., 2000].

To set the $\varepsilon$ data in context, further gradient data are assembled from a number of CTD surveys of the same region. Data from the North Sea project [*Howarth et al*., 1992] are used for stations in the seasonally stratified Northern North Sea, away from the Rhine Outflow/German Bight Regions of Freshwater Influence [e.g., *Simpson et al*., 1993]. Data are taken from the British Oceanographic Data Centre for the seasonally stratified area of the semienclosed Irish Sea [e.g., *Simpson and Rippeth*, 1998]. Data for an open shelf are taken from a cruise on board the RRS *Discovery*, to the Celtic Sea in June 2010, and also for the Malin Shelf Region from the British Oceanographic Data Centre database. The latter data were edited to remove all stations lying within the Scottish Coastal Current, a region of freshwater influence [*Hill and Simpson*, 1989].

## 3. Model to Quantify the Effect of Diapycnal Mixing on Sea Surface $pCO_2$

To quantify the impact of diapycnal mixing on the $pCO_2$ in the surface-mixed layer of a stratified water column, a one-dimensional turbulent diffusion model is derived. A rate equation is defined to describe the changes in $pCO_2$ in terms of the various parameters which influence it; temperature (T), salinity (S), dissolved inorganic carbon (DIC), and alkalinity (ALK), by separating variables [*Mahadevan et al*., 2011]:

$$\frac{\partial pCO_2}{\partial t}=\frac{\partial pCO_2}{\partial T}\frac{\partial T}{\partial t}+\frac{\partial pCO_2}{\partial DIC}\frac{\partial DIC}{\partial t}+\frac{\partial pCO_2}{\partial ALK}\frac{\partial ALK}{\partial t}+\frac{\partial pCO_2}{\partial S}\frac{\partial S}{\partial t} \tag{3}$$

Following *Mahadevan et al*. [2011], the Revelle factors for DIC and alkalinity can be defined as:

$$\gamma=\frac{\Delta pCO_2}{pCO_2}\Big/\left.\frac{\Delta DIC}{DIC}\right|_{ALK=const}$$

and

$$\gamma_A=\frac{\Delta pCO_2}{pCO_2}\Big/\left.\frac{\Delta ALK}{ALK}\right|_{DIC=const} \tag{4}$$

Both of these factors are variable in space and time, with $\gamma$ typically in the range of 8–15 and $\gamma_A$ $-8$ to $-13$ [*Sarmiento and Gruber*, 2006]. Values of $\gamma = 10$ and $\gamma_A = -10$ are taken.

The impact of temperature and salinity on $pCO_2$ is given by *Takahashi et al*. [1993]:

$$\beta=\frac{1}{pCO_2}\frac{\partial pCO_2}{\partial T}=0.0423^{\circ}C^{-1} \tag{5}$$

and

$$\beta_s=\frac{1}{pCO_2}\frac{\partial pCO_2}{\partial S}=0.9^{-1} \tag{6}$$

The above equations provide a framework to quantify the relative contributions of changes in sea surface temperature, salinity, DIC, and alkalinity, due to diapycnal mixing, on the sea surface value of $pCO_2$.

## 4. Turbulent Diffusion Model

In order to examine the impact of diapycnal mixing on the surface value of $pCO_2$, a one-dimensional model is derived in which the property (C) within the surface-mixed layer (depth H) is modified by diapycnal mixing and by a source/sink term which accounts for air-sea interaction and the impact of biological activity. The rate of change of parameter C in the surface-mixed layer is therefore determined by the imbalance between the diapycnal flux ($\partial C/\partial z|_{z=-H}$) and the source/sink term ($S_c$), i.e.,

$$\frac{\partial C}{\partial t} = -\frac{1}{H} K_z \frac{\partial C}{\partial z}\bigg|_{z=-H} + S_c \tag{7}$$

It is assumed that any gradients which arise within the surface-mixed layer, as a consequence of the vertical fluxes, are immediately mixed out, with conditions within the surface-mixed layer remaining homogeneous. In equation (7), $K_z$ is the turbulent diffusion coefficient and is derived from observations of $\varepsilon$ using equation (2). By assuming the thermocline, halocline, and nutricline all coincide with the pycnocline, it is possible to evaluate the different contributions to the change in sea surface $pCO_2$ in response to the diapycnal fluxes driven by turbulent mixing across the pycnocline:

$$\frac{\Delta pCO_2}{pCO_2} = -\frac{K_z \Delta t}{H}\left(\beta \frac{\partial T}{\partial z} + \frac{\gamma}{DIC}\frac{\partial DIC}{\partial z} + \frac{\gamma_A}{ALK}\frac{\partial ALK}{\partial z} + \beta_S \frac{\partial S}{\partial z}\right) + S_T + S_{DIC} + S_{ALK} + S_s \tag{8}$$

In equation (8), the first four terms on the right-hand side represent individual responses of DIC, ALK, T, and S to vertical mixing across the base of the surface-mixed layer and the next four terms represent the individual contributions of sources and sinks of T, DIC, ALK, and S. For the purposes of this paper, we shall calculate the impact of changes on the time scale of a day and so assume that surface fluxes of heat and freshwater can be neglected (i.e., $S_T = S_S = 0$). We also assume that nitrate entering the surface-mixed layer is rapidly used in primary production and that there is no biological mediation of alkalinity, and by implication that there is no source or sink for alkalinity ($S_{ALK} = 0$). Equation (8) then reduces to:

$$\frac{\Delta pCO_2}{pCO_2} = -\frac{K_z \Delta t}{H}\left[\left(\beta \frac{\partial T}{\partial z} + \beta_S \frac{\partial S}{\partial z}\right) + \frac{\gamma_A}{ALK}\frac{\partial ALK}{\partial z} + \frac{\gamma}{DIC}\frac{\partial DIC}{\partial z}\right] + S'_{DIC}$$

On the basis that mixing and restratification processes occur on faster time scales than the reequilibrium time scale for $CO_2$, it is further assumed that there is no exchange of $CO_2$ across the sea surface. It is reasonable to assume, for temperate shelf seas at this time of the year, that there is no light limitation on primary productivity and so the term $S'_{DIC}$, which represents the DIC sink resulting from primary production fuelled by the introduction of nitrate into the surface-mixed layer, can be written:

$$S'_{DIC} = -\frac{K_z \Delta t}{H}\left[\frac{\gamma}{DIC} R_{pp} \frac{\partial NO_3}{\partial z}\right] \tag{9}$$

where $R_{pp}$ represents net primary production via the biological uptake ratio of dissolved inorganic carbon (DIC) to inorganic nitrogen ($NO_3^-$), often assumed to be equivalent to the Redfield ratio, DIC:$NO_3^-$ of 106:16, i.e., $R_{pp} = 6.625$. Through incorporation of equation (9), (8) becomes:

$$\frac{\Delta pCO_2}{pCO_2} = -\frac{K_z \Delta t}{H}\left[\left(\beta \frac{\partial T}{\partial z} + \beta_S \frac{\partial S}{\partial z}\right) + \frac{\gamma}{DIC}\left(\frac{\partial DIC}{\partial z} + R_{pp}\frac{\partial NO_3}{\partial z}\right) + \frac{\gamma_A}{ALK}\frac{\partial ALK}{\partial z}\right] \tag{10}$$

By then assuming that the thermocline, halocline, nitracline, and DIC gradient are colocated, and that the water column is essentially two layered (i.e., a homogeneous surface layer overlying a homogeneous bottom layer, which are separated by a thermocline thickness $\Delta z$), equation (10) can be further simplified to:

$$\Delta pCO_2 = -\frac{K_z . pCO_2 . \Delta t}{H . \Delta z}\left((\beta \Delta_z T + \beta_s \Delta_z S) + \frac{\gamma}{DIC}\left(\Delta DIC + R_{pp}\Delta_z NO_3\right) + \frac{\gamma_A}{ALK}\Delta_z ALK\right) \tag{11}$$

Equation (11) thus provides a framework to quantify the relative impact of the change in each parameter, over a time step $\Delta t$, due to vertical mixing, on the sea surface $pCO_2$. The estimated contributions are based on the observed difference ($\Delta_z$) in each parameter value between the surface-mixed layer and the deep water, with the assumption of a two-layer structure and a $NO_3^-$/DIC sink associated with primary production being located within the surface layer.

## 5. Results

To assess the relative impacts of the diapycnal temperature, salinity, alkalinity, DIC, and nitrate fluxes on the sea surface $pCO_2$, the contribution of the individual terms in equation (11) will first be considered. In temperate shelf seas, the salinity, and temperature gradients tend to oppose each other, i.e., while the water temperature decreases with depth, the salinity increases. Vertical mixing will therefore generally result in the surface-mixed layer becoming cooler and saltier. The impact of the changing salinity on $pCO_2$ will therefore tend to compensate for the impact of changing temperature via their effect on $CO_2$ solubility. For the case, where the impact of the mixing-induced cooling on sea surface $pCO_2$ is exactly compensated for by the effect of increasing salinity (at constant DIC and ALK):

$$\frac{\partial S}{\partial z} = -\frac{\beta}{\beta_s}\frac{\partial T}{\partial z} \tag{12}$$

where $-\beta/\beta_s = -0.047$.

An assessment of the relative impacts of the temperature and salinity changes brought about by vertical mixing on the surface $pCO_2$ is made through plotting the sea surface to seabed salinity difference against the temperature difference for each of the stations given in Table 1 (Figure 3). Figure 3 shows that a number of stations lie above the line, illustrating the ratio of the parameters in equations (5) and (6). At these stations, the impact of the increase in the salinity of the SML due to the diapycnal salt flux on the $pCO_2$ (at constant T, DIC, and ALK), will be greater than the impact of the accompanying SML temperature (at constant S, DIC, and ALK). At these stations, the combined impacts of the salt and heat fluxes yield a net increase in the surface $pCO_2$ (at constant DIC and ALK).

Conversely for stations which lie below the theoretical line, the effect of the negative heat flux dominates and the net result is a reduction in $pCO_2$. For the limited number of stations given in Table 1, half lie above the line (i.e., the rise in salinity has a bigger impact than the fall in temperature due to vertical mixing), while half lie below. Data collected during the summer for a whole series of stations across the Celtic Sea, Malin shelf, Irish, and North Seas are presented in Figure 4. The results show a wide distribution with salinity fluxes dominating in a few in the semienclosed North Sea and western Irish Sea, while the salinity structure is inverted (more saline water overlying less saline deep water) for a significant number of the stations on the Malin shelf and in the Celtic Sea. In these cases, the salt and heat fluxes will be in the same direction and, as a result, will combine to reduce $pCO_2$. Overall, the impact of the diapycnal salt flux on the surface $pCO_2$ appears to be as important as the diapycnal heat flux across significant areas of seasonally stratified temperate shelf seas.

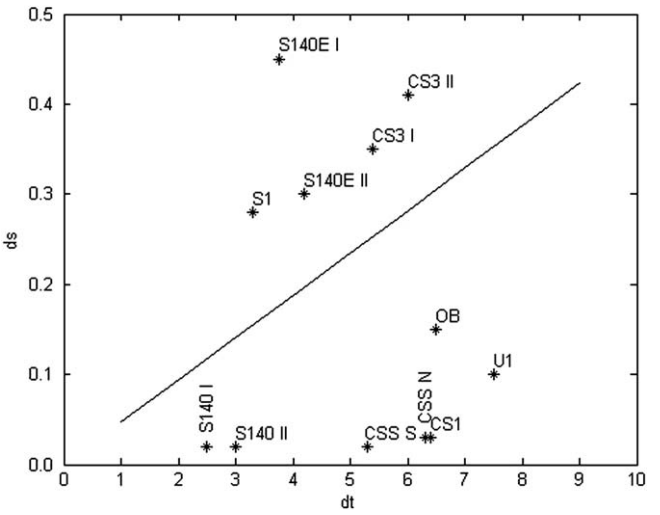


**Figure 3.** The ratio of $-\Delta S/\Delta T$ for a number for the stations shown in Figure 1. The diagonal line represents the ratio of $\beta/\beta_s$. For points lying above the line, the impact on sea surface $pCO_2$ of the diapcynal salt flux into the surface-mixed layer will exceed the cooling of the surface layer, which results from the same turbulent mixing event.

The alkalinity distribution within shelf seas is commonly related to salinity through TA-S plots [e.g., *Cai et al.*, 2010]. These plots are formed through the linear regression of alkalinity against salinity, and so the alkalinity is given by:

$$ALK = ALK^0 + bS \tag{13}$$

where $ALK^0$ is the riverine ($S = 0$) end-member alkalinity value and b is the slope. Linear regression of observations from continental shelf seas not influenced by freshwater input, and so similar to those considered here, with surface-mixed layer salinities, $S > 33$, yields values of $b \approx 30$–$60$, e.g., for the English Channel [*Kitidis et al.*, 2012] and

for the continental shelf areas along the eastern seaboard of the North America [*Cai et al.*, 2010]. A similar salinity-based linear regression parameterization is adopted in the current generation of ecosystem models [e.g., *Wakelin et al.*, 2012]. Differentiating equation (13) gives:

$$\frac{\partial ALK}{\partial z} = b.\frac{\partial S}{\partial z} \tag{14}$$

One can therefore reduce the term describing the relative contributions of the diapycnal salt and alkalinity fluxes to:

$$\left(\beta_s \frac{\partial S}{\partial z} + \frac{\gamma_A}{ALK}\frac{\partial ALK}{\partial z}\right) = \frac{\partial S}{\partial z}\left(\beta_s + b.\frac{\gamma_A}{ALK}\right) \tag{15}$$

Assuming typical English Channel values for ALK = 2400 [e.g., *Kitidis et al.*, 2012], $\gamma_A = -10$ and b = 30–60 indicate that the impact of the alkalinity flux will partly compensate for the impact of the salt flux accounting for between 12% and 24% of the impact of the salt flux on $pCO_2$.

Due to the low resolution of nutrient measurements from bottle samples, the nutrient gradient is often estimated through correlation with the temperature gradient [e.g., *Rippeth et al.*, 2009; *Williams et al.*, 2013a]. It is therefore useful to compare the impact of the diapycnal nitrate flux (as a $CO_2$ sink) on $pCO_2$ relative to the impact of the cooling of the SML, i.e., balancing the terms:

$$\left(\frac{\gamma}{DIC}R_{pp}\frac{\partial NO_3^-}{\partial z}\right) = \left(\beta\frac{\partial T}{\partial z}\right)$$

i.e.,

$$\left(\frac{\partial NO_3^-}{\partial z}\right) = \frac{DIC.\beta}{\gamma R_{pp}}\left(\frac{\partial T}{\partial z}\right) \tag{16}$$

Assuming the phytoplankton C:N uptake ratio, $R_{pp}$ equivalent to the Redfield ratio (6.625), a reported deep water DIC = 2100 mmol $m^{-3}$ and $\gamma$ =10, equation (15) thus yields a ratio of:

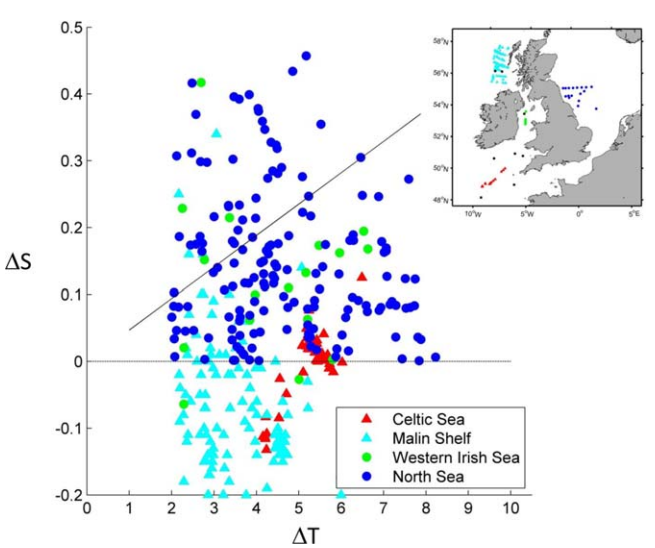


**Figure 4.** The ratio of $-\Delta S/\Delta T$ for a stations across the Northwest European shelf seas. The geographic distribution of the stations is shown in the insert map. The diagonal line represents the ratio of $\beta/\beta_s$. For points lying above the line, the impact on sea surface $pCO_2$ of the diapcynal salt flux into the surface-mixed layer will exceed the cooling of the surface layer which results from the same turbulent mixing event.

$$\frac{DIC.\beta}{\gamma R_{C:N}} \approx 1.34$$

This may be compared to the typically observed ratios of nitrate to temperature gradients from Northwest European seasonally stratified shelf seas of 2.1–3.3 (examples of fits are given in Figure 5). In other words, the impact of diapycnal nitrate flux alone on $pCO_2$, through the DIC sink created by the primary production it fuels, significantly exceeds the impact of the change in solubility driven by the cooling of the SML from the diapycnal heat flux, in these oceanographic settings.

The combined impacts of the diapycnal fluxes of the different parameters on $pCO_2$ are shown for the stations listed in Table 1 (Figure 6a). Here, it is assumed that $R_{pp}$ = 6.625 and that

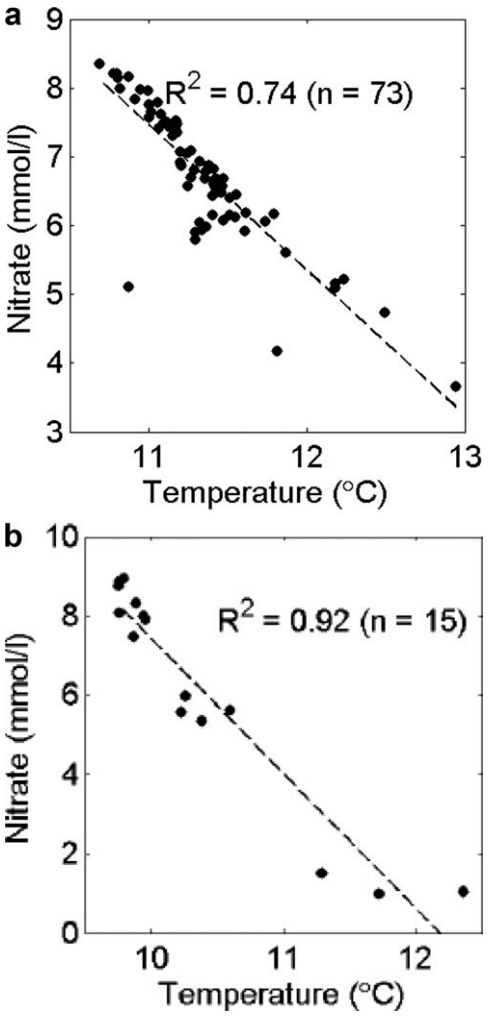


**Figure 5.** Temperature-nitrate relationships for (a) CS3 using measurements taken over a 24 h period starting on the 5th August 2003 and (b) S140E using measurements taken over a 24 h period starting on the 15th July 1996.

the $\Delta_z$DIC = 100 mmol $m^{-3}$, with the latter value based on reported summer values for seasonally stratified Northwest European shelf seas [*Bozec et al*., 2006; *Kitidis et al*., 2012]. In all cases, the impacts of the DIC flux and the compensatory nitrate flux dominate with smaller contributions resulting from the heat, salt, and alkalinity fluxes. This calculation predicts a daily increase in $pCO_2$ of up to 6 μatm $d^{-1}$. The largest net flux is obtained for the mid-Celtic Sea location CS1, with other significant fluxes estimated for the other Celtic Sea locations. In all cases the impact of large DIC fluxes (individually this flux would result in a rise in $pCO_2$ of between 1 and 15 μatm $d^{-1}$) is somewhat buffered by the compensatory impacts of the $NO_3^-$ flux, with smaller impacts arising from the heat, salt, and alkalinity fluxes. In consequence the impact of diapycnal DIC flux greatly reduced.

The impact of the nitrate flux is determined by the C:N assimilation ratio of the phytoplankton within the subsurface chlorophyll maximum (i.e., $R_{pp}$). Available observations indicate *overconsumption* of carbon relative to nitrogen in nitrate depleted regions such as the surface-mixed layer, in the summer. The resultant C:N ratio is found to be larger than the Redfield ratio in many cases, with the observed estimates reported to vary over a range of 8.7–30 [*Smabrotto et al*., 1993; *Toggweiller*, 1993; *Engel et al*., 2002; *Schartau et al*., 2007] in nitrate depleted regions which include estimates of 8.7–9.5 for the SCM in the seasonally stratified English Channel [*Kitidis et al*., 2012]. The impact of an increased value of $R_{pp}$ (assumed to be 10 for illustrative purposes) is shown in Figure 6b. The results show a decline in the impact of diapycnal mixing on account of an increase in the compensatory effect of the diapycnal nitrate flux-induced primary production on the sea surface $pCO_2$.

The sensitivity of the impact of vertical mixing on $pCO_2$ to the value of $R_{pp}$ is demonstrated using average gradient and $\varepsilon$ data for midshelf stations S1 and high mixing station CS1 (Figure 7). As with the previous calculations, an assumed value of $\Delta_z$ DIC = 100 mmol $m^{-3}$ is taken. $R_{pp}$ is varied over the range 6.625–30, in accordance with published estimates. The results show that over this range of values of $R_{pp}$ selected the impact of diapycnal mixing varies from increasing sea surface $pCO_2$ by 1 μatm $d^{-1}$ to reducing it by 4 $\mu$atm $d^{-1}$. The value of $R_{pp}$ is therefore a key determinate of both the direction and magnitude of the impact of vertical mixing on the sea surface $pCO_2$. In other words, for typical parameter values from temperate shelf seas, the degree to which the diapycnal DIC flux, which acts to increase the sea surface value of $pCO_2$, is compensated for by the accompanying $NO_3^-$ flux which, through fuelling primary production, creates at DIC sink, is very sensitive to the value for $R_{pp}$.

Toward the left-hand side of Figure 7, a situation occurs where the combined impacts of the DIC and $NO_3^-$ fluxes exactly cancel (e.g., $\Delta_z$DIC = $R_{pp}\Delta_z NO_3$). In this case, the net impact of vertical mixing is determined

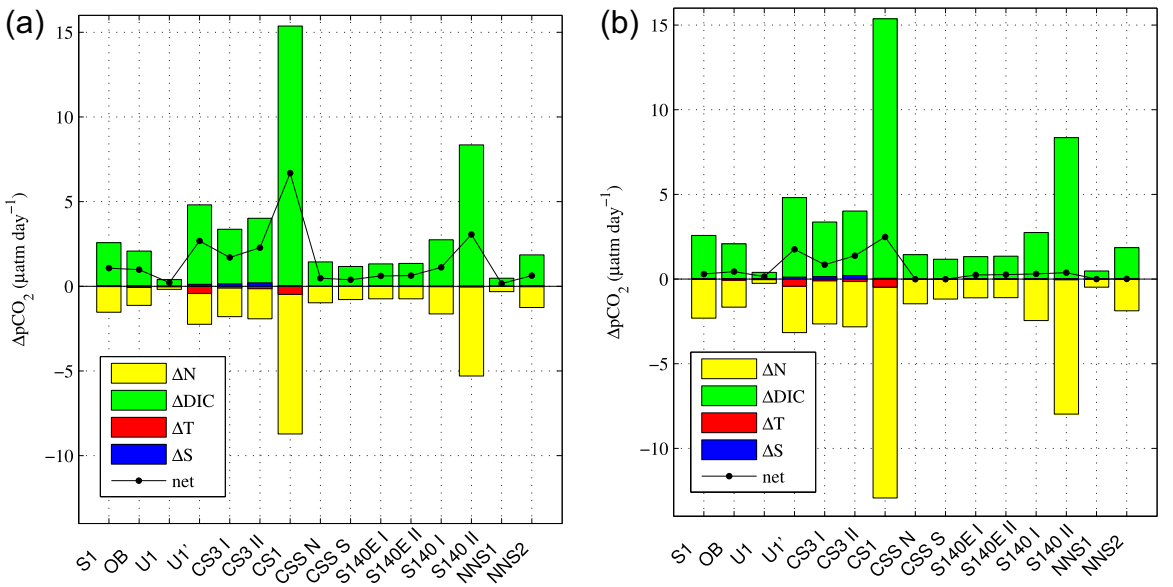


**Figure 6.** Estimates of the individual impacts of the different parameters on the sea surface $pCO_2$ as a consequence of diapycnal mixing. In Figure 6a, a value of $R_{pp} = 6.625$ is assumed whilst in Figure 6b, a value of $R_{pp} = 10$ is assumed. The impact of the alkalinity flux is too small to be visible.

by the balance of hydrographic fluxes, as shown in Figure 8. This comparison of the estimates for the different stations highlights the key role of the physical environment in determining the impact of the diapycnal mixing on surface $pCO_2$. While the pycnocline averaged values for the rate of dissipation $\varepsilon$ for S1, S140E, and NNS_I are all similar, the impact of the diapycnal fluxes varies considerably. This variability is largely on account of the difference surface-mixed layer depth at the different sites (which ranges from 10 to 40 m), and therefore in dilution volume of the surface-mixed layer. While the environmental conditions are almost identical for NNS_I and NNS_II, the pycnocline averaged value of $\varepsilon$ is nearly 3 times larger for NNS_II, hence driving larger fluxes, and producing a significantly larger impact on $pCO_2$.

## 6. Discussion

We have investigated the impact of diapycnal mixing on surface $pCO_2$ in temperate seasonally stratified shelf seas. Numerous synoptic surveys of these regions have identified them as a significant sink for atmospheric $CO_2$ during the period of seasonal stratification [e.g., *Thomas et al.*, 2004; *Borges et al.*, 2005; *Cai et al.*, 2005; *Chen and Borges*, 2009; *Evans et al.*, 2012; *Kitidis et al.*, 2012]. The air-sea $\Delta pCO_2$, and hence the ocean $pCO_2$, is a key parameter in the estimation of air-sea $CO_2$ fluxes and ultimately the magnitude of $CO_2$ sink.

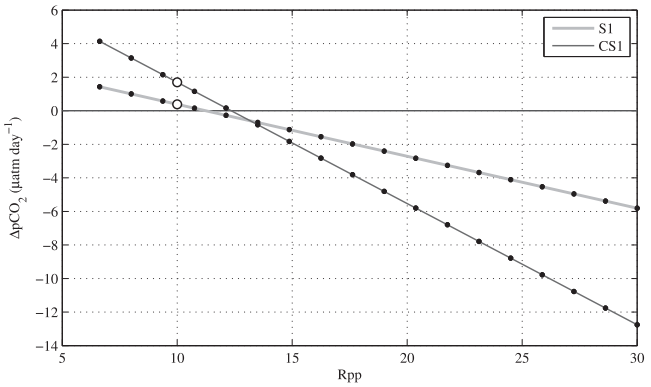


**Figure 7.** The sensitivity of the net impact of diapycnal mixing on sea surface $_pCO_2$ using values of $K_z$, H, and gradients using the observed values from an average midshelf station, S1, and from a high dissipation station, CS1.

Following the spring bloom primary production in these regimes is largely confined to the SCM, which is sustained through the diapycnal flux of limiting nutrient across the seasonal thermocline [*Sharples et al.*, 2001]. Recent measurements suggest that the deficit in surface $pCO_2$ relative to that of the atmosphere, during the summer, is inversely correlated to chlorophyll-*a* integrated over the SML, rather than the surface chlorophyll [*Kitidis et al.*,

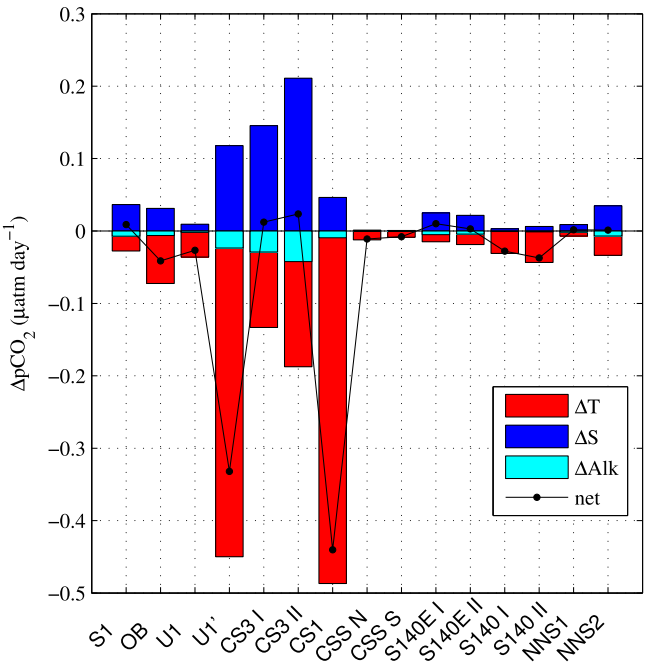


**Figure 8.** As Figure 6, but for the situation when the net impact of the nitrate and DIC fluxes on the sea surface $pCO_2$ in zero.

2012]. This result implies that the subsurface chlorophyll maximum plays a key role in determining the uptake of atmospheric $CO_2$ in the summer in these regions. *Evans et al.* [2012] report estimates of air-sea $CO_2$ fluxes across the continental shelf to the west of Canada, which show significant enhancement over the continental shelf break, a region of enhanced diapycnal mixing, when compared to mixing levels over the continental shelf. These observations therefore provide qualitative evidence linking the surface $pCO_2$ to the diapycnal mixing rate.

To investigate the impact of diapycnal mixing on surface $pCO_2$, we have used a one-dimensional turbulent diffusion model in which primary productivity is only limited by nitrate availability, and the plankton C:N uptake rate is assumed to be constant. The model is used to quantify the net impact of the diapycnal fluxes of the limiting nutrient (nitrate in this case), heat, salt, alkalinity, and DIC on $pCO_2$ for a range of contrasting locations in the Northwest European shelf seas. This framework provides a useful method for identifying the key processes responsible for determining sea surface $pCO_2$.

The model predicts that the largest contribution to the sea surface $pCO_2$ change results from the diapycnal DIC flux and the DIC sink created by the primary production fuelled by the compensatory $NO_3^-$ flux. A key parameter in the diffusion model presented is therefore the C:N assimilation ratio by phytoplankton over the SCM ($R_{pp}$). Figure 7 shows that over the range of $R_{pp}$ values reported in the literature (as reported in section 5) the predicted daily change in sea surface $pCO_2$, as a result of mixing, ranges from an increase of 6 $\mu$atm $d^{-1}$ to a decrease of $<20$ $\mu$atm $d^{-1}$. The temporal variability in sea surface $pCO_2$ implied from the analysis is therefore sufficient to explain the reported diurnal variability observed in similar shelf sea hydrographic regimes. For example, *Dai et al.* [2009] report an observed diurnal variability of 10–15 $\mu$atm in the stratified South China Sea, while 30–40 $\mu$atm changes are reported for the English Channel [*Litt et al.*, 2010; *Bozec et al.*, 2011].

There is significant spatial variability in the estimated impact of diapycnal mixing on sea surface $pCO_2$. The smallest impacts are estimated for midshelf locations with relatively deep surface-mixed layers (e.g., NSS_I and U1). The highest impacts are found for the Celtic Sea station, CS1, where high values for $\varepsilon$ have been attributed to the presence of a seamount, and at stations close to the continental shelf break. In these cases the observed enhancement of dissipation is attributed to the interaction between the tidal flow and local topography.

Although the daily estimates for $\Delta pCO_2$ due to diapycnal mixing are generally modest, the integrated diapcynal flux of DIC and nitrate into the surface-mixed layer during summer (e.g., 120 days) will result in a significant perturbation in the sea surface $pCO_2$, potentially leading to significant fluxes of $CO_2$ across the air-sea interface. It is unlikely that these changes would be detectable in the lower-resolution synoptic surveys of the air-sea $\Delta pCO_2$ gradient reported in the literature thus adding to the uncertainty in current estimates of the magnitude of the $CO_2$ sink for these locations.

There is significant temporal variability in the implied impact of the diapycnal fluxes on sea surface $pCO_2$ even over the short time scales used in this study. For example, at U1 the estimated impact is negligible for much of the 24 h period of the observations. The exception is the 2 h period with the enhanced $\varepsilon$ resulting from the penetration of the bottom mixed layer into the thermocline. At this time, the impact on sea surface $pCO_2$ is over an order of magnitude larger (shown as U1′ in Figures 6 and 7). Thus, overall the resultant impact of diapycnal mixing on the sea surface $pCO_2$ is strongly influenced by the relatively short period of enhanced diapcynal mixing. The enhanced $\varepsilon$ observed close to the shelf break leads to relatively large estimated changes in the sea surface $pCO_2$ (e.g., at S140 and CSSB). Here diapcynal mixing is thought to result from turbulence generated by the dissipation of an internal tide and associated internal solitary waves, and so one would expect levels of mixing, and therefore diapycnal fluxes, to vary over spring-neap time scales as well as the tidal cycle.

A second key hydrodynamic factor in the estimation of the impact of mixing on surface $pCO_2$ is the SML depth. At S140, although $<\varepsilon>$ is larger close to the spring tides, the SML is also deeper at this time. Hence, the impact of the enhanced diapycnal mixing is diminished due to the larger SML volume. Similar results were obtained for midshelf locations. For example, similar values of $<\varepsilon>$ are found at S1, S140E, and the NNS_I, but the impact on the sea surface $pCO_2$ varies by a factor of 5 on account of the varying SML depths, which ranged from 10 to 40 m. *Lincoln et al*. [2014] report the impact of the windy conditions associated with the passage of a midlatitude cyclone on the surface-mixed layer in the seasonally stratified western Irish Sea. The enhanced winds associated with the passage of the weather system resulted in the SML deepening from 15 to 40 m, thus implying the entrainment of a significant quantity of deep water into the surface-mixed layer. For several days, following the event periods of enhanced shear, across the thermocline, coincident with the alignment of the wind with the inertially rotating surface current, were observed. The presence of such shear spikes have been observed to significantly enhanced diapycnal fluxes, with temporally averaged fluxes observed to increase by between 4 and 20 times during periods with shear spikes [*Burchard and Rippeth*, 2009; *Lenn et al*., 2011; *Williams et al*., 2013b]. Coincident with this significant wind-driven perturbation in $pCO_2$, the air-sea exchange of $CO_2$ will also be greatly accelerated on account of the quadratic dependence of the gas exchange coefficient on wind speed [e.g., *Ho et al*., 2006]. The sensitivity of the surface $pCO_2$ to both the surface-mixed layer depth and dissipation, within the thermocline, coupled with the accelerated air-sea gas exchange during windy periods, imply that episodic wind events could have a substantial impact on the seasonally integrated air-sea $CO_2$ flux away from regions of rough topography.

The analysis has identified the key biogeochemical parameter in determining the magnitude, and potentially the direction, of air-sea $CO_2$ fluxes as the ratio of the phytoplankton C:N assimilation in the region of the subsurface chlorophyll maximum. Here we have assumed a constant ratio but demonstrated the impact by varying the value over the wide range of observed C:N values (referenced in the results section). Because different groups of phytoplankton have differing C:N ratios, which vary depending on cell growth conditions, the observed wide range of C:N assimilation ratios most likely reflects the functional composition of the subsurface phytoplankton community. Key questions therefore arise as to the impact of both the spatial and temporal variability in mixing on the C:N assimilation ratio, i.e., on phytoplankton composition, and ultimately on the whole ecosystem functioning. For the purposes of this study, we have neglected the impact of biological mediation of alkalinity on $pCO_2$. While on the time scales considered the impact will be generally negligible, pelagic calcification during, for example, a large coccolithophore bloom, may lead to a significant decrease in alkalinity and thus increase in $pCO_2$.

In conclusion, the analysis presented here, which covers a wide range of contrasting locations in the seasonally stratified Northwest European shelf seas, has identified diapycnal mixing as a potentially important process in determining both the magnitude and direction of air-sea $CO_2$ exchange during the period of seasonal stratification, and therefore in determining the seasonally integrated air-sea $CO_2$ flux. The key role of biological activity within the subsurface chlorophyll maximum builds on the conclusion of *Sharples et al*. [2001] and *Kitidis et al*. [2012] that remote sensing-based estimates underestimate productivity implying that they will also miss a key contribution to the net air-sea $CO_2$ flux. The sensitivity of $pCO_2$ to diapycnal mixing, coupled with the large observed spatial and temporal variability in mixing rates has important consequences for estimating shelf wide carbon budgets and in particular implies the need for both high spatial

and high temporal resolution synoptic surveys of $\Delta pCO_2$ for accurate flux estimation. The analysis also identifies a number of key parameters which coupled hydrodynamic-ecosystems models need to accurately represent in order to be able to predict the uptake of atmospheric carbon dioxide in these regions, which have been identified as significant $CO_2$ sinks. These include the surface-mixed layer depth, both the spatial and temporal variability of mixing rates across the thermocline and hence the evolution of the surface chlorophyll maximum (including accurate representation of the variability in the C:N uptake ratio). In particular the analysis suggests that, while the kinetic energy budget of the Northwest European shelf seas is dominated by the tide, episodic wind events may well be a key process in determining seasonally integrated $CO_2$ fluxes over these regions.

**Acknowledgments**
This work was funded through NERC standard grant NE/F002858 and CandyFlos consortium NE/G010986. B.J.L. and C.A.J.W. where funded through NERC PhD studentships. Data used here were collected from the RV Prince Madog and NERC Research vessels Challenger and Discovery. Additional data were provided by the British Oceanographic Data Centre and processed by Oliver Way.

## References

Artioli, Y., J. C. Blackford, M. Butenschon, J. T. Holt, S. L. Wakelin, H. Thomas, A. V. Borges, and J. I. Allen (2012), The carbonate system in the North Sea: Sensitivity and model validation, *J. Mar. Syst.*, *102–104*, 1–13.

Bauer, J. E., W.-J. Cai, P. A. Raymond, T. S. Bianchi, C. S. Hopkinson, and P. A. G. Regnier (2013), The changing carbon cycle of the coastal ocean, *Nature*, *504*, 61–71.

Borges, A. V., B. Delille, and M. Frankignoulle (2005), Budgeting sinks and sources of $CO_2$ in the coastal ocean: Diversity of ecosystem counts, *Geophys. Res. Lett.*, *32*, L14601, doi:10.1029/2005GL023053.

Bozec, Y., H. Thomas, L.-S. Schiettecatte, A. V. Borges, K. Elkaly, and H. J. W. Baar (2006), Assessment of the processes controlling seasonal variations of dissolved inorganic carbon in the North Sea, *Limnol. Oceanogr. Methods*, *51*(6), 2746–2762.

Bozec, Y., et al. (2011), Diurnal to inter-annual dynamics of $pCO_2$ recorded by a CARIOCA sensor in a temperate coastal ecosystem (2003–2009), *Mar. Chem.*, *126*, 13–26.

Burchard, H., and T. P. Rippeth (2009), Generation of bulk shear spikes in shallow stratified tidal seas, *J. Phys. Oceanogr.*, *39*, 969–985.

Cai, W.-J., M. Dai, and Y. Wang (2005), Air-sea exchange of carbon dioxide in ocean margins: A province based synthesis, *Geophys. Res. Lett.*, *33*, L12603, doi:10.1029/2006GL026219.

Cai, W.-J., X. Hu, W.-J. Huang, L.-Q. Jiang, Y. Wang, T.-H. Peng, and X. Zhang (2010), Alkalinity distribution in the western North Atlantic Ocean margins, *J. Geophys. Res.*, *115*, C08014, doi:10.1029/2009JC005482.

Chen, C. T. A., and A. V. Borges (2009), Reconciling opposing views on carbon cycling in the coastal ocean: Continental shelves as sinks and near-shore ecosystems as sources of atmospheric $CO_2$, *Deep Sea Res., Part II*, *56*, 578–590.

Dai, M., Z. Lu, W. Zhai, B. Chen, Z. Cao, K. Zhou, W.-J. Cai, and C. T. A. Chen (2009), Diurnal variations of surface seawater $pCO_2$ in contrasting coastal environments, *Limnol. Oceanogr. Methods*, *54*(3), 735–745.

Engel, A., S. Goldthwait, U. Passow, and A. Alldredge (2002), Temporal decoupling of carbon and nitrogen dynamics in a mesocosm diatom bloom, *Limnol. Oceanogr.*, *47*, 753–761.

Evans, W., B. Hales, P. G. Strutton, and D. Iansen (2012), Sea-air $CO_2$ fluxes in the western Canadian coastal ocean, *Prog. Oceanogr.*, *101*, 78–91.

Fernand, L., K. Weston, T. Morris, N. Greenwood, J. Brown, and T. Jickells (2013), The contribution of the deep chlorophyll maximum to primary production in a seasonally stratified shelf sea, the North Sea, *Biogeochemistry*, *113*, 153–166, doi:10.1007/s10533-013-9831-7.

Green, J. A. M., J. H. Simpson, S. A. Thorpe, and T. P. Rippeth (2010), Observations of internal tidal waves in the isolated seasonally stratified region of the western Irish Sea, *Cont. Shelf Res.*, doi:10.1016/j.csr.2009.11.004.

Gibson, C. E., B. M. Stewart, and R. J. Gowen (1997), A synoptic study of nutrients in the North-west Irish Sea, *Estuarine Coastal Shelf Sci.*, *45*, 27–38.

Hickman, A. E., C. M. Moore, J. Sharples, M. I. Lucas, G. H. Tilstone, V. Krivtsov, and P. M. Holligan (2012), Primary production and nitrate uptake within the seasonal thermocline of a stratified shelf sea, *Mar. Ecol. Prog. Ser.*, *463*, 39–67.

Hill, A. E., and J. H. Simpson (1989), On the interaction of thermal and haline fronts—The Islay Front revisited, *Estuarine Coastal Shelf Sci.*, *28*(5), 495–505.

Ho, D. T., C. S. Law, M. J. Smith, P. Schlosser, M. Harvey, and P. Hill (2006), Measurements of air-sea gas exchange at high wind speeds in the Southern Ocean: Implications for global parameterisations, *Geophys. Res. Lett.*, *33*, L16611, doi:10.11029/12006GL026817.

Howarth, M. J., et al. (1992), Seasonal cycles and their spatial variability, in *Understanding the North Sea System*, edited by H. Charnock et al., pp. 5–25, Chapman and Hall, London.

Inall, M. I., T. P. Rippeth, and T. J. Sherwin (2000), The impact of non-linear waves on the dissipation of internal tidal energy at a shelf break, *J. Geophys. Res.*, *105*, 8687–8705.

Kitidis, V., et al. (2012), Seasonal dynamics of the carbonate system in the Western English Channel, *Cont. Shelf Res.*, *42*, 30–40.

Knight, P. J., M. J. Howarth, and T. P. Rippeth (2002), Inertial currents in the northern North Sea, *J. Sea Res.*, *47*, 269–284.

Lenn, Y. D., T. P. Rippeth, C. P. Old, S. Bacon, I. Polyakov, V. Ivanov, and J. Hölemann (2011), Intermittent intense turbulent mixing under ice in the Laptev Sea continental shelf, *J. Phys. Oceanogr.*, *41*(3), 531–547.

Litt, E. J., N. J. Hardman-Mountford, J. C. Blackford, A. Goodman, G. F. Moore, D. G. Cummings, and M. Butenschon (2010), Biological control of $pCO_2$ at station L4 in the Western English Channel over 3 years, *J. Plankton Res.*, *32*, 621–629.

Liu, X., K. Furuya, T. Shiozaki, T. Masuda, T. Kodama, M. Sato, H. Kaneko, M. Nagasawa, and I. Yasuda (2013), Variability in nitrogen sources for new production in the vicinity of the shelf edge of the East China Sea in summer, *Cont. Shelf Res.*, *61–62*, 23–30.

MacKinnon, J. A., and M. C. Gregg (2005), Near inertial waves on the New England Shelf: The role of evolving stratification, turbulent dissipation and bottom drag, *J. Phys. Oceanogr.*, *35*, 2408–2424.

Mahadevan, A., A. Tagiabue, L. Bopp, A. Lenton, L. Memery, and M. Levy (2011), Impact of episodic vertical fluxes on sea surface $pCO_2$, *Philos. Trans. R. Soc. A*, *369*, 2009–2025.

Osborn, T. R. (1980), Estimates of the local rate of vertical diffusion from dissipation measurements, *J. Phys. Oceanogr.*, *10*, 83–89.

Palmer, M. R., T. P. Rippeth, and J. H. Simpson (2008), An investigation of internal mixing in a seasonally stratified shelf sea, *J. Geophys. Res.*, *113*, C12005, doi:10.1029/2007JC004531.

Palmer, M. R., M. E. Inall, and J. Sharples (2013a), The physical oceanography of Jones Bank: A mixing hotspot in the Celtic Sea, *Prog. Oceanogr.*, *117*, 9–24.

Palmer, M. R., J. A. Polton, M. E. Inall, T. P. Rippeth, J. A. M. Green, J. Sharples, and J. H. Simpson (2013b), Variable behaviour in pycnocline mixing over shelf seas, *Geophys. Res. Lett.*, *40*, 161–166, doi:10.1029/2012GL054638.

Richardson, K., A. W. Visser, and F. B. Pedersen (2000), Subsurface phytoplankton blooms fuel pelagic production in the North Sea, *J. Plankton Res.*, *22*, 1663–1671.
Rippeth, T. P. (2005), Mixing in seasonally stratified shelf seas: A shifting paradigm, *Philos. Trans. R. Soc. A*, *363*, 2837–2854.
Rippeth, T. P., and M. E. Inall. (2002), Observations of the internal tide and associated mixing across the Malin Shelf, *J. Geophys. Res.*, *107*(C4), doi:10.1029/2000JC000761.
Rippeth, T. P., M. R. Palmer, J. H. Simpson, N. R. Fisher, and J. Sharples (2005), Thermocline mixing in summer stratified continental shelf seas, *Geophys. Res. Lett.*, *32*, L05602, doi:10.1029/20004GL022104.
Rippeth, T. P., P. Wiles, M. R. Palmer, J. Sharples, and J. Tweddle (2009), The diapycnal nutrient flux and shear-induced diapycnal mixing in the seasonally stratified western Irish Sea, *Cont. Shelf Res.*, *29*, 1580–1587.
Sambrotto, R. N., G. Savidge, C. Robinson, P. Boyd, T. Takahashi, D. M. Karl, C. Langdon, D. Chipman, J. Marra, and L. Codispoti (1993), Elevated consumption of carbon relative to nitrogen in the surface ocean, *Nature*, *363*, 248–250.
Sarminto, J. L., and N. Gruber (2006), *Ocean Biogeochemical Dynamics*, 528 pp., Princeton Univ. Press, New York.
Schartau, M., A. Engel, J. Schroter, S. Thoms, C. Volker, and D. Wolf-Gladrow (2007), Modelling carbon overconsumption and the formation of extracellular particulate organic carbon, *Biogeosciences*, *4*, 433–454.
Sharples, J., and P. Tett (1994), Modelling the effect of physical variability on the midwater chlorophyll maximum, *J. Mar. Res.*, *52*, 219–238.
Sharples, J., C. M. Moore, T. P. Rippeth, P. M. Holligan, D. J. Hydes, N. R. Fisher, and J. H. Simpson (2001), Phytoplankton distribution and survival in the thermocline, *Limnol. Oceanogr.*, *46*(3), 486–496.
Sharples, J., O. N. Ross, B. E. Scott, S. P. R. Greenstreet, and H. Fraser (2006), Interannual variability in the timing of stratification and the spring bloom in the North-western North Sea, *Cont. Shelf Res.*, *26*, 733–751.
Sharples, J., et al. (2007), Spring-Neap modulation of internal tide mixing and vertical nutrient fluxes at a shelf edge in summer, *Limnol. Oceanogr. Methods*, *52*, 1735–1757.
Simpson, J. H., and J. Hunter (1974), Fronts in the Irish Sea, *Nature*, *250*, 404–406.
Simpson, J. H., and T. P. Rippeth (1998), Non-conservative nutrient fluxes from budgets for the Irish Sea, *Estuarine Coastal Shelf Sci.*, *47*, 707–714.
Simpson, J. H., and J. P. Tinker (2009), A test of the influence of tidal stream polarity on the structure of turbulent dissipation, *Cont. Shelf Res.*, *29*, 320–332.
Simpson, J. H., W. G. Bos, F. Schirmer, A. J. Souza, T. P. Rippeth, S. E. Jones, and D. Hydes (1993), Periodic stratification in the Rhine Region of Freshwater Influence, *Oceanol. Acta*, *16*, 23–32.
Stacey, M. T., T. P. Rippeth, and J. D. Nash (2012), Turbulence and stratification in Estuaries and Coastal Seas, in *Treatise on Estuarine and Coastal Science*, vol. 2, edited by R. Uncles and S. Monismith, pp. 9–36, Elsevier, Amsterdam.
Takahashi, T., J. Olafsson, J. Goddard, D. Chipman, and S. C. Sutherland (1993), Seasonal variation of $CO_2$ and nutrient in the high-latitude oceans: A comparative study, *Global Biogeochem. Cycles*, *7*, 843–878.
Thomas, H., Y. Borac, K. Elkalay, and H. J. W. Baar (2004), Enhanced open ocean storage of $CO_2$ from shelf sea pumping, *Science*, *304*, 1005–1008.
Toggweiler, J. R. (1993), Carbon overconsumption, *Nature*, *363*, 210–211.
van Haren, H., L. Mass, J. T. R. Zimmerman, H. Ridderinkhof, and H. Malschaert (1999), Strong inertial currents and marginal internal wave stability in the central North Sea, *Geophys. Res. Lett.*, *26*, 2993–2996.
van Leeuwen, S. M., J. van der Molen, P. Ruardij, L. Fernand, and T. Jickells (2013), Modelling the contribution of deep chlorophyll maxima to annual production in the North Sea, *Biogeochemistry*, *113*, 137–152, doi:10.1007/s10533-012-9704-5.
Wakelin, S. L., J. T. Holt, J. C. Blackford, J. I. Allen, M. Butenschon, and Y. Artioli (2012), Modelling the carbon fluxes of the northwest European continental shelf: Validation and budgets, *J. Geophys. Res.*, *117*, C05020, doi:10.1029/2011JC007402.
Walsh, J. J. (1991), Importance of continental margins in the marine biogeochemical cycling of carbon and nitrogen, *Nature*, *350*, 53–55.
Weston, K., L. Fernand, D. K. Mills, R. Delahunty, and J. Brown (2005), Primary production in the deep chlorophyll maximum of the central North Sea, *J. Plankton Res.*, *27*(9), 909–922.
Williams, C. A. J., J. Sharples, M. Green, C. Mahaffey, and T. P. Rippeth (2013a), The maintenance of the subsurface chlorophyll maximum in the western Irish Sea, *Limnol. Oceanogr. Methods*, *3*, 61–73.
Williams, C. A. J., J. Sharples, C. Mahaffey, and T. P. Rippeth (2013b), Wind driven pulses of nutrients to phytoplankton in stratified shelf seas, *Geophys. Res. Lett.*, *40*, 5467–5472, doi:10.1002/2013GL058171.